X-ray photoemission of $YbInCu_4$

S. Schmidt* and S. Hüfner
Fachrichtung 7.2—Experimentalphysik, Universität des Saarlandes, D-66041 Saarbrücken, Germany

F. Reinert
Experimentelle Physik II, Universität Würzburg, D-97074 Würzburg, Germany

W. Assmus
Physikalisches Institut, Universität Frankfurt, D-60054 Frankfurt, Germany
(Received 21 January 2005; published 23 May 2005)

We present temperature-dependent Al-K_α ($\hbar\omega$=1486.6 eV) x-ray photoemission spectroscopy (XPS) measurements on $YbInCu_4$, which has—dependent on small variation in the stoichiometry—a particular first-order phase transition in the range of 40 K at ambient pressure. The qualitative analysis of the phase transition monitored by Yb 4*f* and Yb 4*d* XPS data shows a steep change of the Yb valence, which has been reported for the bulk material by various thermodynamic and other spectroscopic measurements. In contrast, this phase transition has not been unambiguously observed in highly surface-sensitive ultraviolet photoemission spectroscopy experiments with excitation energies below 100 eV. The XPS data support previous conclusions that surface effects suppress the first-order phase transition in $YbInCu_4$ in the region close to the sample surface. An estimate of the spatial extent of this region as well as an assessment of the existing photoemission data on $YbInCu_4$ taken with photon energies from $\hbar\omega$=20 eV to $\hbar\omega$=5950 eV are given.

DOI: 10.1103/PhysRevB.71.195110 PACS number(s): 71.20.Eh, 71.27.+a, 71.28.+d, 79.60.−i

I. INTRODUCTION

Similar to the $\alpha \rightarrow \gamma$ phase transition in cerium metal ("Kondo volume collapse"[1–3]) there exists a first-order phase transition in the ytterbium compound $YbInCu_4$,[4–6] which shows a sudden change of the lattice constant in connection with a change of the Yb valence. In contrast to Ce, the volume of the $YbInCu_4$ crystal *increases* in going below the transition temperature $T_a \approx 40$ K.[7–12] With a relative change of about 0.2% the effect on the lattice constant is much smaller than for the $\alpha \rightarrow \gamma$ transition in Ce; the valence change in $YbInCu_4$ of the order of 0.1—as estimated from various thermodynamic and spectroscopic techniques—is comparatively small but significant.

Although photoemission spectroscopy (PES) with photon energies in the VUV range (ultraviolet PES: UPS) is widely used to study the electronic properties of strongly correlated rare earth compounds, the investigation of the valence transition in $YbInCu_4$ exhibits some principal questions concerning the implication of surface effects to PES data from intermediate valent Yb compounds: at photon energies of $\hbar\omega$ =43, 120, or 21 eV the temperature dependence of the PES data shows only a smooth change of the Yb valence over a large temperature range while a sharp steplike transition, as it is observed in volume sensitive measurements, is lacking.[13–15] Furthermore, the Yb valence extracted from PES is smaller than, e.g., the values determined by x-ray absorption spectroscopy at the L_{III} edge (XAS).[7,16] At a photon energy of $\hbar\omega \approx 9$ keV, XAS used in the transmission mode can be regarded as a bulk-sensitive tool, almost free from complications caused by surface effects. To the contrary, in PES measurements using excitation energies in the VUV range, the small mean free path of the photoelectrons (e.g., in the range of 5 Å for $\hbar\omega$=43 eV) results in a small information depth for electronic states close to the Fermi level.

The principal differences of the XAS and the UPS results on intermediate valent Yb compounds can be explained by the existence of a subsurface zone with physical properties different from those of the bulk.[10,13,17] This subsurface zone should be characterized by a lattice constant relaxing over several unit cells from the true bulk value to a larger value at the crystal surface. The spatial structure of this ordered subsurface region should strongly influence the observed Yb-valence: (1) bulk Yb-valence below the subsurface region with unrelaxed/undistorted bulk, (2) decreased valence (more divalent than bulk) in the still long range ordered intermediate buffer zone with "relaxed" or increasing lattice constant towards the surface, i.e., with a larger Yb ion radius between the small bulk value and the large surface value (purely divalent), and (3) purely divalent outermost surface Yb atoms (due to reduced coordination). Such a significant surface relaxation has been observed for Yb and other metallic systems;[18–21] recent experiments with high-resolution XPS[22–25] have demonstrated the influence of the probing depth on the PES results for several systems including nonmetallic compounds. In addition, intermediate-valent Yb compounds are extremely sensitive to inner and outer distortions such as external pressure, magnetic field, and substitution or defects, resulting in significant changes of the physical properties.[5,10,26–29] In the case of $YbInCu_4$ it is well known that such distortions are able to broaden or even completely suppress the first-order transition.[30]

In this paper we present temperature-dependent XPS laboratory experiments at a photon energy of $\hbar\omega$ =1486.6 eV (Al-K_α), for which the information depth on the ytterbium 4*f* and 4*d* states is larger than for VUV energies.[31–33] These measurements have been performed on

TABLE I. The inelastic mean free path (IMFP) λ from the "universal curve" (Ref. 47) (experimentally from overlayer method) and calculated for $YbInCu_4$ using the TPP-2 formula (Ref. 31) for states close to the Fermi level.

	UPS	XPS
Photon energy $\hbar\omega$ (eV)	43	1486.6
IMFP (experimental) (Å)	4	20
IMFP (calculated) (Å)	3–7	20–40

the identical samples investigated by UPS in Ref. 13. A brief account of these experiments has been reported in Ref. 34. There exist two other spectroscopic measurements of the valence change of $YbInCu_4$ with energies between the UPS experiments (21 eV, 43 eV) and the XAS experiments (8900 eV) apart from the XPS experiments with 1487 eV for which the original results obtained under laboratory conditions were reported by Reinert *et al.*[34] and the details of the experiments are given here. These are RIXS (resonant inelastic x-ray scattering) experiments by Dallera *et al.*[35] ($\hbar\omega$ = 8900 eV) and a HXPS (hard x-ray photoemission spectroscopy) experiment by Sato *et al.*[36] that both require synchrotron radiation. Thus $YbInCu_4$, with its changing physical properties in the crystal surface region, has been investigated spectroscopically with photon energies ranging from $\hbar\omega$ = 20 eV to $\hbar\omega$ = 8900 eV, meaning that one has data that are surface sensitive ($\hbar\omega$ = 40 eV) and other data ($\hbar\omega$ = 8900 eV) that are bulk sensitive. Therefore, after a presentation of our results we shall give a comparison of the merits and problems of the spectroscopic results obtained with the different photon energies.

II. EXPERIMENTAL

Different from most of the photoemission data published on $YbInCu_4$, the XPS data presented in this paper have been measured with a laboratory system, the SES 200 analyzer of a SCIENTA ESCA 200, equipped with a monochromatized x-ray anode (Al-K_α, $\hbar\omega$ = 1486.6 eV). The data were taken in normal emission using a net energy resolution of ΔE = 600 meV. The typical accumulation times for a single valence band spectrum and for the 4*d* core-level was 3.5 and 1 h, respectively. The sample temperature could be controlled on a resistively heated open-cycle cryostat over a temperature range from T = 10 K up to room temperature. The $YbInCu_4$ samples were Bridgman-grown single crystals cut to a size of $3\times3\times3$ mm^3. To prepare clean surfaces the samples were cleaved *in situ* at a base pressure of 5×10^{-11} mbar using a cleavage post. Freshly prepared surfaces were comparatively rough but—as monitored by core-level XPS—free from oxygen or carbon contaminations. Prior to the temperature series, the samples were cleaved at different starting temperatures, to rule out any influence from surface degradations or a possible cracking prior to cleavage. Note that, due to the higher information depth (cf. Table I), the XPS spectra are much less sensitive to surface degradation processes than the UPS data.[13]

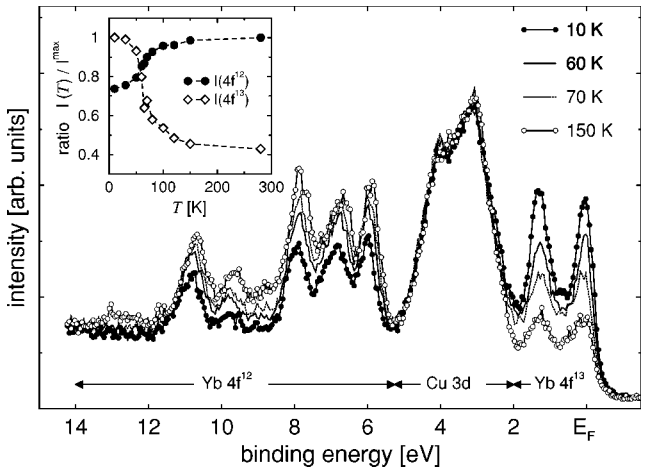

FIG. 1. The x-ray photoemission spectra (XPS) of the Yb 4*f* states at four temperatures from T = 10 K < T_a to T = 150 K > T_a, with the transition temperature $T_a \approx 52$ K. The inset shows the temperature dependence of the integrated spectral weight of the $4f^{12}$ (●) and the $4f^{13}$ contribution (◇), without any background correction; the spectra are normalized to the intensity of the Cu 3*d* band.

III. XPS RESULTS

The spectral features typical of the 4*f* states from an intermediate-valent Yb compound are depicted in Fig. 1, which shows XPS valence band data of $YbInCu_4$ at four different temperatures. Due to the different photoemission final states the 4*f* spectrum is split into two distinct parts,[37] a "trivalent" multiplet ranging from 12 to 6 eV binding energy, corresponding to the two-hole $4f^{12}$ final state,[38] and a "divalent" part (labeled $4f^{13}$), appearing as a spin-orbit doublet close to the Fermi energy.[39,40] The $4f^{13}$ part contains some unresolved temperature-independent contributions from the merely divalent Yb ions of the top-most surface layer that are clearly resolved only in UPS data. The intense feature between these two 4*f* contributions is the Cu 3*d* band, the intensity of which does not change with temperature.[13,17] The 4*f* spectra clearly show a characteristic dependence on the sample temperature with opposite direction for the $4f^{12}$ and $4f^{13}$ contributions: increasing the temperature leads to an increasing intensity of the $4f^{12}$ multiplet, whereas the intensity of the divalent $4f^{13}$ doublet decreases at the same time. A plot of the non-background-corrected integrated intensities demonstrates this for the temperatures from T = 10 K to 280 K (see inset of Fig. 1). The maximum slope of the temperature dependence lies around the transition temperature T_a, i.e., in the range between $T \approx 50$ K and 60 K (ΔT = 10 K).[12]

The Yb valence v_{Yb} or the hole occupation number $n_h = v_{\mathrm{Yb}} - 2$ can be determined directly from the intensity ratio of the two 4*f* contributions:

$$n_h = \left(1 + \frac{13}{14}\frac{I_{4f}^{13}}{I_{4f}^{12}}\right)^{-1}, \qquad (1)$$

where I_{4f}^{12} and I_{4f}^{13} are the integrated spectral weights for the trivalent and the divalent 4*f* part, respectively.[41] This method of determining the hole occupation is similar to the one used

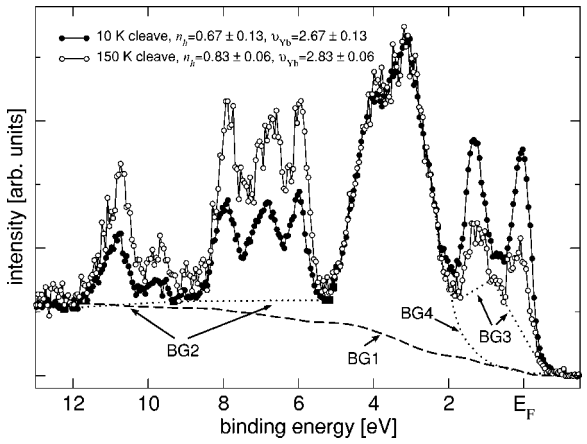

FIG. 2. The determination of n_h (and v_{Yb}) and choice of background for the reference spectra at $T=10$ and $T=150$ K normalized on the Cu $3d$ integral (see text for details).

in XAS,[42] except that at least in the valence band PE spectra, the I_{4f}^{12} and I_{4f}^{13} spectral contributions do not overlap and we have to use a factor of $\frac{13}{14}$ to include the $4f$ multiplicity. For the case of PES on the $4d$ core level, which will be discussed later, the procedure is like in XAS with overlapping structures for 3+ and 2+ contributions. The measurement of a series of spectra at different temperatures can be accelerated, if one measures complete $4f$ reference spectra only at a few selected temperatures T_{ref} (preferably above and below the transition temperature T_a, see Fig. 2) and restricts the measurement at the other temperatures to the $4f^{13}$ doublet close to the Fermi energy and—for normalization—the Cu $3d$ band. Because of the fixed relation between divalent and trivalent spectral weight[43] one is able to reconstruct the temperature dependence of the occupation number n_h by

$$n_h(T) = 1 - \frac{1 - n_h(T_{\mathrm{ref}})}{I_{4f}^{13}(T_{\mathrm{ref}})} \times I_{4f}^{13}(T). \qquad (2)$$

The complete $4f$ spectrum was measured at the beginning and end of each series of spectra to rule out possible surface degradation effects.

An exact quantitative determination of the Yb valence requires a careful consideration of the non-$4f$ background. Since the background contribution cannot be determined exactly and might differ for various cleaves, we use another approach for the analysis of the data by simply confining the results to the maximum and minimum possible values of the extracted intensities $I_{4f}^{12}(T)$ and $I_{4f}^{13}(T)$ by using maximum and minimum choices for the corresponding background correction. The backgrounds for the trivalent and the divalent part of the spectra have to be chosen independently. As a maximum intensity for the $4f^{12}$ part (minimum background) we take the integrated spectral weight from $E_B=13$ to 5.3 eV after subtraction of a "Shirley background" for the complete spectrum (see BG1 in Fig. 2, long-dashed line). The maximum background is determined by a sequence of linear connections of the minimum intensities at 12, 9, and 5 eV in the $4f^{12}$ spectrum at $T=10$ K (BG2, dotted line).

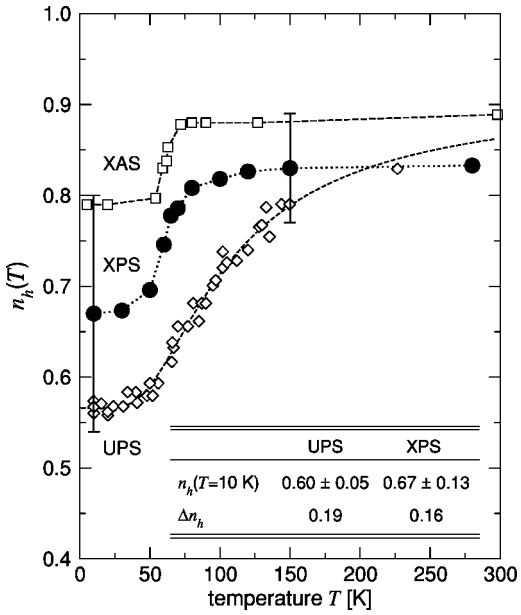

FIG. 3. The temperature dependence of the $4f$ hole occupation number $n_h(T)=v_{\mathrm{Yb}}(T)-2$, determined differently by XPS ($\hbar\omega=1486.6$ eV, ●), UPS from Ref. 13 ($\hbar\omega=43$ eV, ◇), and XAS from Ref. 7 (L_{III} edge measurement, □). The table shows the low temperature n_h values and $\Delta n_h = n_h(150\ \mathrm{K}) - n_h(10\ \mathrm{K})$. The "error bars" indicate the resulting temperature dependence with the maximum and minimum non-$4f$ background used in the analysis. The black dots give the mean values.

For the divalent $4f^{13}$ doublet we again take two linear interpolations between the local minimum intensities at 2, 1, and −0.5 eV as the highest background, but now from the spectrum at $T=150$ K where the $4f^{13}$ weight is small (see BG3 in Fig. 2). For the estimate of the minimum background we extrapolate the Cu $3d$ band towards E_F, following a Gaussian profile (see BG4 in Fig. 2). All four backgrounds are considered as temperature *in*dependent.

With these background corrections one gets a maximum and minimum value of both the I_{4f}^{12} and I_{4f}^{13} for each temperature. To map out the complete range of all reasonably possible hole occupation numbers $n_h(T)$ we combine these maximum and minimum intensities crosswise according to Eq. (1). In Fig. 3 we confine this range by "error bars" at 10 K and 150 K and plot the mean value of both extrema by filled circles (●) for all investigated temperatures. From the spectra in Fig. 2 we have pinned the temperature behavior at two reference temperatures and thereby get $n_h(150\ \mathrm{K})=0.83$ and $n_h(10\ \mathrm{K})=0.67$; the range indicated as bars in Fig. 3 arises from the choice of the upper and lower limits for the subtracted background as described above. Within these "error bars" we get the relationship $n_h^{\mathrm{XAS}} > n_h^{\mathrm{XPS}} > n_h^{\mathrm{UPS}}$ for the n_h values for the three different methods. Note that these "error bars" do not correspond to a scatter of the n_h values but display two $n_h(T)$ limiting curves with the highest and the lowest reasonable hole occupation numbers at each temperature, respectively. As a consequence of the considerable intensity change of the $4f$ spectra over a narrow temperature range (see inset Fig. 1), all of these curves show a steep change of the hole occupation number n_h at the transition

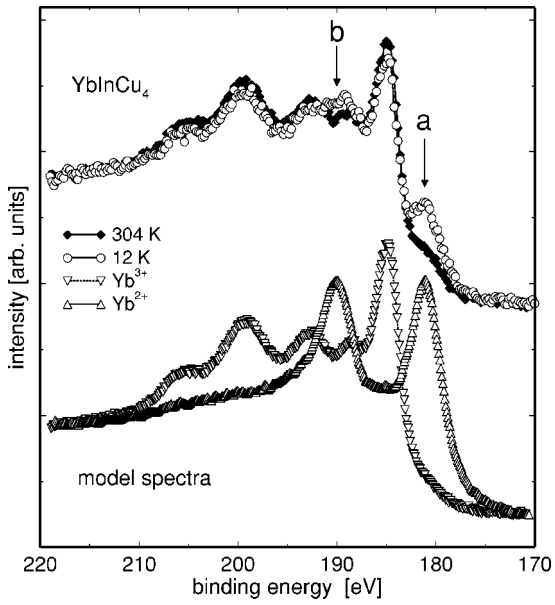

FIG. 4. The decomposition method of the 4*d* core-level of the intermediate valent compound $YbInCu_4$ into divalent and trivalent model spectra; contributions are for the high- and low-temperature case. Similar to the case of the valence band, the divalent model spectrum ($\triangle$, Yb^{2+}) still contains an unresolvable divalent but temperature-independent contribution from the surface Yb atoms.

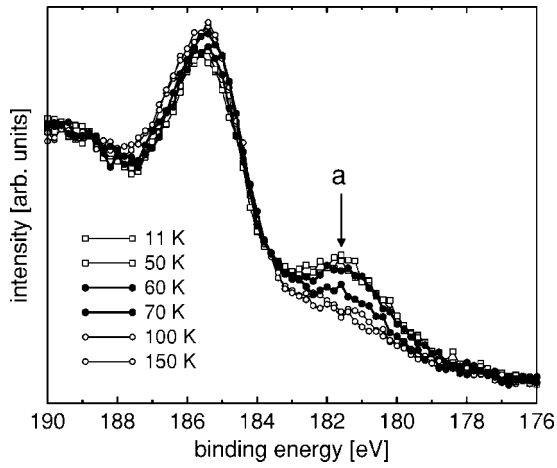

FIG. 5. The low E_B-part of the Yb 4*d* core-level spectra for selected temperatures, normalized to the total integral. There is a sudden increase of divalent spectral weight between 70 and 50 K, while the spectra below 50 and above 100 K exhibit only a small variation of the $4d_{5/2}$-peak (see also Fig. 6).

temperature $T_a \approx 52$ K, in agreement with the XAS, RIXS, and HXPS data, although in the latter two experiments at a slightly lower temperature.[12] For temperatures clearly above T_a the hole occupation values of both XPS and XAS rapidly reach constant values.

In addition to the measurements of the 4*f* states in the valence band we have chosen the Yb 4*d* core level[44,45] for tracking the temperature dependence of the hole occupation number. The basic idea of the analysis is illustrated in Fig. 4. At the bottom of Fig. 4 we show the 4*d* spectra for two materials representing the two valence limits of Yb-based intermetallics, i.e., the purely divalent states found in Yb metal (Yb^{2+}) and the trivalent states in oxidized $YbInCu_4$ (Yb^{3+}). The remaining two curves (above) show the high- and low-temperature spectra from the 4*d* temperature series (see also Fig. 5) of $YbInCu_4$.

The structures labeled a and b indicate the position of the most prominent divalent features in the 4*d* spectra. Thus, in the intermediate valent $YbInCu_4$ the change of n_h with temperature can—in a similar way as with the 4*f* states—be observed in the 4*d* spectra, and we can analyze each 4*d* spectrum by its decomposition into the di- and trivalent contribution in the measured range. Quantifying the intensity ratio of the two corresponding parts results in the n_h values.

Although there is no structured non-4*d* spectral contribution underlying the core spectra—in contrast to the valence band with non-4*f* contributions from the conduction band and Cu 3*d* states—the quantification of the intensity ratio and consequently n_h is complicated by the fact that the spectral contributions overlap and are not well separated as in the case of the $4f^{12}$ and $4f^{13}$ states in the valence band. Furthermore, there is also an unresolvable divalent contribution to the 4*d* spectra from the surface Yb atoms as in the case of the valence band. Therefore, in our analysis we concentrate on the integral change of the divalent part ($\propto 1-n_h$) of the intermediate valent 4*d* spectra. To get its temperature dependence it is sufficient to evaluate the low binding energy part of the divalent 4*d* contribution ($4d_{5/2}$ peak, feature a in Fig. 5) located at $E_B \approx 181.6$ eV. In several temperature cycles across the transition temperature T_a we have observed a full return of the divalent spectral weight in the 4*d* core-level spectra. Therefore, we conclude that the formerly observed smooth valence change in UPS is not a result of a repeated temperature cycle through the phase transition as it was assumed by Moore *et al.*[46] From the ratio of normalized di- and trivalent contribution in the intermediate valent spectra, we can estimate a low-temperature hole occupancy of $n_h \approx 0.76$. Since this absolute n_h value is less reliable than the 4*f* results for the reasons stated above, we restrict ourselves to the discussion of the qualitative 4*d* temperature behavior and compare the results to those from 4*f* XPS, UPS, and XAS in the following.

Figure 3 shows our results from XPS on the 4*f* states together with the UPS results ($\hbar\omega = 43$ eV) for the n_h values from Ref. 13 and those from XAS from Ref. 7. In Fig. 6, we have added the results for the change in $n_h(T)$ from the analysis of the 4*d* emission to the data already given in Fig. 3 in order to demonstrate the temperature dependence. We have expanded the curves to the same total range in n_h to allow a more direct comparison of the different results. Both XPS methods, the analysis of the total changes of divalent contributions in the 4*f* and in the 4*d* spectra, exhibit the same qualitative behavior. On the other hand, there are significant differences between XPS and UPS results, although the data have been measured on identical samples: the temperature dependence of the XPS values unambiguously shows a significantly *steeper* change around the transition temperature $T_a \approx 52$ K, whereas the change in the UPS results is smooth and extended over a large temperature range. The similarity between the mean XPS values and the XAS results is quite

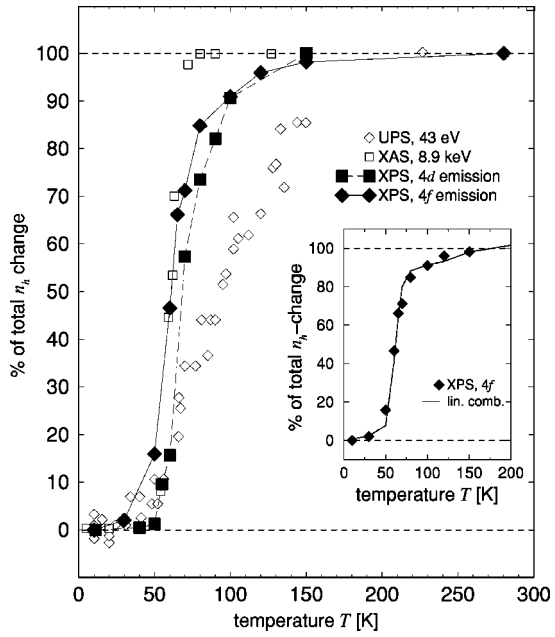

FIG. 6. The comparison of the Yb valence transition of $YbInCu_4$ as monitored by 4*d* and 4*f* emission scaled to the same range. The curve for the 4*d* spectra describes the temperature behavior of peak a denoted in Fig. 5. The underlying $n_h(T)$ curves (UPS and XAS data, open symbols) from Fig. 3 are scaled to the same relative range. Inset: the transition as observed in 4*f* emission can be modeled by a linear combination of the XAS and UPS $n_h(T)$-values with the ratio 4:1.

striking, although a slight broadening of the transition is present in the XPS results.

IV. DISCUSSION OF UPS AGAINST XPS RESULTS

The most obvious difference between XPS and UPS lies in the used photon energy for the excitation. For electronic states close to the Fermi level and core levels with low binding energies the kinetic energy E_{kin} of the respective photoelectrons is comparable with the photon energy $\hbar\omega$, i.e., $E_{kin} \approx 1.5$ keV and ≈ 1.3 keV for our XPS data (4*f* and 4*d*), and $E_{kin} \approx 40$ eV for the UPS data. Electron-electron scattering processes make the inelastic mean free path (IMFP) of a photoelectron strongly dependent on its kinetic energy. As a result the photoemission information depth ID differs typically by a factor of ≈ 5 between VUV ($\hbar\omega = 43$ eV) and Al-K_α ($\hbar\omega = 1486.6$ eV) excitation. Table I gives the relevant theoretical and experimental numbers for the two cases considered. From Fig. 3 we find that all mean hole occupation numbers n_h have values between those from XAS and UPS ($n_h^{\mathrm{XAS}} > n_h^{\mathrm{XPS}} > n_h^{\mathrm{UPS}}$) over the temperature range of the transition, while the information depths ID ($\approx 3\lambda$) of the three methods are ordered in the same way ($\mathrm{ID}^{\mathrm{XAS}} > \mathrm{ID}^{\mathrm{XPS}} > \mathrm{ID}^{\mathrm{UPS}}$). With this knowledge about the different information depths the assumption of a structurally relaxed subsurface zone[13,17] is able to explain the observed qualitative and quantitative differences in the temperature dependence of $n_h(T)$ for the three experimental methods. In this subsurface zone, the transition that results in the "bulk" 4*f* spectra is suppressed as it can also be observed in distorted bulk material.[30] In $YbInCu_4$ already a lattice distortion of 1–2% is known to suppress the sharp transition in the bulk and to shift the transition temperature T_a to higher values.[28]

From the calculated inelastic mean free path at the different photoelectron energies one can estimate the thickness of the subsurface zone if we assume an exponential damping ($3\lambda \approx 95\%$ damping) of the photoelectron current through the solid:[33] the resulting XPS (Al-K_α) information depth of ~ 90 Å must be significantly larger than the width of the distorted subsurface zone. However, there is a small broadening of the transition in the XPS data compared to the steep valence change in the XAS data. By a decomposition of the $n_h^{\mathrm{XPS}}(T)$ into the $n_h^{\mathrm{XAS}}(T)$ and $n_h^{\mathrm{UPS}}(T)$ curves, which shall represent mere bulk and subsurface zone behavior, one can extract a $\sim 20\%$ contribution from the subsurface zone to the XPS signal (see inset of Fig. 6). This contribution equals a thickness of the subsurface zone of about one to three lattice constants.

The structural model of a relaxed subsurface layer different from the bulk together with the different surface sensitivities between UPS and XPS data is also able to explain the differences in the observed $n_h(T)$ curves: the UPS temperature dependence of n_h in $YbInCu_4$ is similar to the gradual change of $n_h(T)$, as it was determined by PES measurements on the intermediate valent compounds $YbAgCu_4$ or $YbAl_3$,[43,48] and by XAS L_{III} edge measurements on various Yb compounds, which can be explained by the predictions of the single-impurity Anderson model (SIAM).[42] From this point of view the temperature dependence of the UPS data that represent the subsurface region could be explained within the SIAM by a single Kondo phase with one Kondo temperature $T_{\mathrm{K}} \approx 200$ K. This Kondo temperature T_{K} would be temperature independent without a change at the bulk transition temperature T_a (short-dashed line in the UPS data in Fig. 3). The XPS data would mainly correspond to the bulk properties with a low T_{K} phase with $T_{\mathrm{K}} < T_a$, which is observed at high temperatures $T \gg T_a$, and a high T_{K} phase ($T_{\mathrm{K}} > T_a$) observed at low temperatures $T \ll T_a$. Within these phases the temperature dependence is too small to be observed and analyzed in detail.

V. COMPARISON OF RELATIVE MERITS OF UPS, XPS, AND HXPS DATA

In addition to the UPS, XPS, and XAS data there are now also RIXS data ($\hbar\omega = 8900$ eV) and in particular HXPS data available where the latter lead themselves to an interesting comparison because at least in the valence band one now has similar PES data sets excited with photons ranging from $\hbar\omega = 21$ eV to $\hbar\omega = 5950$ eV, thus with very different escape depths ranging from ~ 5 to ~ 50 Å. Figure 7 compares valence band PES spectra taken with $\hbar\omega = 5950$ eV and $\hbar\omega = 1487$ eV. They have been normalized by attributing to the Yb $4f_{7/2}$ states (the 4*f* states at the Fermi energy) the same intensity. The two spectra sets are similar, however not identical. In the $4f^{13}$ part of the spectrum ($4f_{7/2}$ and $4f_{5/2}$ structure near the Fermi energy) the temperature dependence is

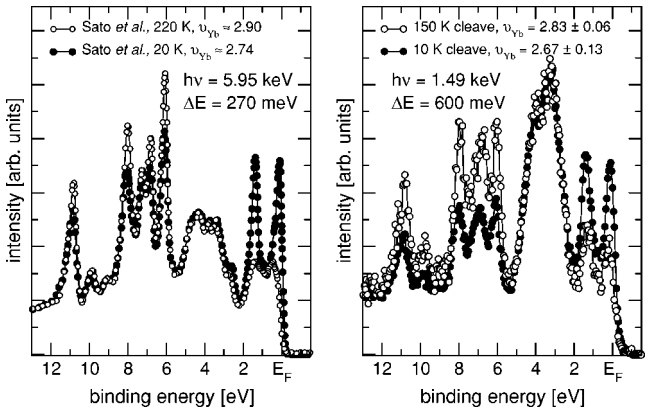

FIG. 7. The comparison of HXPS data (Ref. 36) at $T=20$ K and $T=220$ K with XPS data (this work). The XPS data (right) were taken on samples cleaved and measured at the same temperature ($T=10$ K and $T=150$ K).

more pronounced in the HXPS data than in the XPS data. However, in the $4f^{12}$ final state this trend is reversed. The Cu 3*d* structure is smaller in the HXPS data than in the XPS data, which is a simple cross-section effect. There is no temperature dependence in the Cu 3*d* spectra which shows that the normalization procedures have been done correctly. If the valencies are evaluated in the same way from the HXPS and the XPS 4*f* valence bands, we get the results shown in Table II. Unfortunately, the HXPS data of the Yb 3*d* level do not carry an explicit error. From our experience, we think that an error bar of $\delta v_{\mathrm{Yb}}=\pm 0.05$ seems reasonable. Using this error, all the data for XPS and HXPS just given, which use only PES data, overlap within these error bars. If we plot the XAS, XPS, RIXS, and HXPS data in the same way as used in Fig. 6, namely taking the total temperature-dependent valence change as 100%, then we get the plot in Fig. 8, which shows that the four data sets are not too different. This indicates that already the XPS experiment measures predominantly the bulk properties of $YbInCu_4$.

While the Yb valence and its temperature dependence $v_{\mathrm{Yb}}(T)$ are a very important property, there are other spectroscopic features of a mixed valent compound like $YbInCu_4$ which deserve attention. This is, e.g., the energy and width of the $4f_{7/2}$ peak related to the Kondo resonance—the central property in the single impurity model—which seems to be the model of choice to analyze data in mixed valent systems. Looking at the data in Fig. 7, one would judge that the $4f_{7/2}$ line is positioned directly at the Fermi energy and that its width is resolution limited (300 meV in the HXPS and 600 meV in the XPS data). In order to get more insight into

TABLE II. Comparison of Yb valencies from XPS and HXPS experiments.

Method	Level	$v_{\mathrm{Yb}}^{T\gg T_a}$	$v_{\mathrm{Yb}}^{T\ll T_a}$
HXPS	4*f*	2.75±0.16 (220 K)	2.68±0.14 (20 K)
XPS	4*f*	2.83±0.06 (150 K)	2.67±0.13 (10 K)
HXPS	3*d*	~2.90 (220 K)	~2.74 (20 K)
XPS	4*d*	2.74±0.05 (150 K)	2.92±0.015 (12 K)

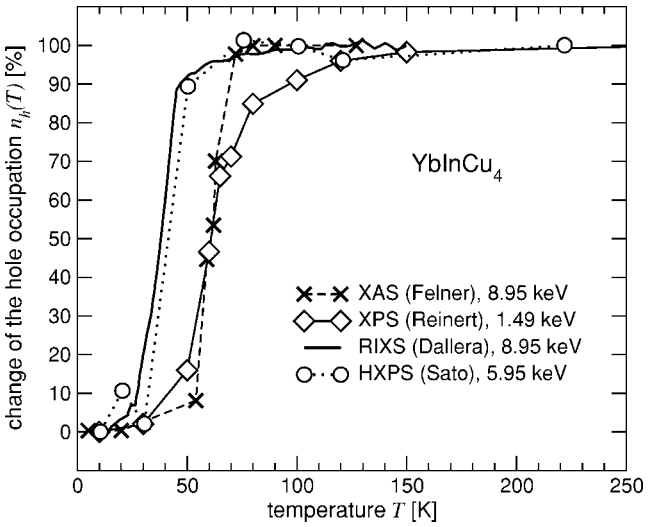

FIG. 8. The normalized temperature dependence of the Yb hole occupancy $n_h(T)$ as obtained from 4*f* XPS (Ref. 34), 3d HXPS (Ref. 36), RIXS (Ref. 35), and XAS (Ref. 7). The RIXS and HXPS experiments have been performed on "42 K samples," the XAS and XPS experiments on "52 K samples."

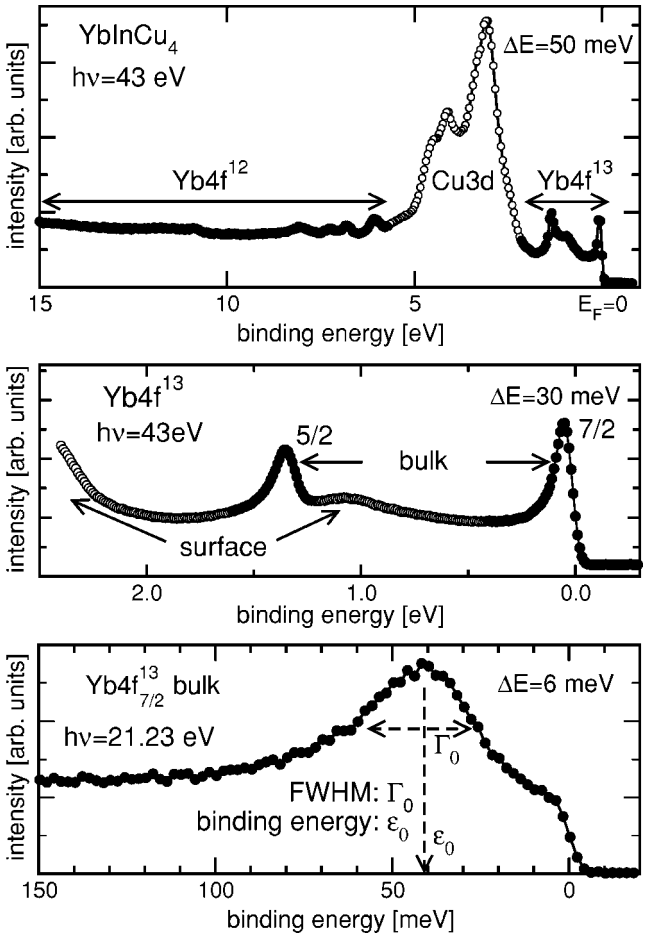

FIG. 9. The high resolution UPS spectra of $YbInCu_4$, taken with energy resolutions of $\Delta E=50$, 30, and 6 meV, respectively.

this problem, Fig. 9 shows UPS data with different energy resolutions ranging from 50 to 6 meV.

Only in the very high resolution UPS data is it possible to obtain the exact position and width for the $4f_{7/2}$ peak ($\sim$40 meV). In the case of ytterbium the contributions from the subsurface zone and the surface to the spectra are clearly separated, which facilitates the analysis of these data. The comparison of the data in Figs. 7 and 9 indicates that both techniques, namely HXPS and XPS on the one hand and UPS on the other hand, have their merits in the investigation of a system like $YbInCu_4$ and have to be used with respect to the problem to be solved.

VI. CONCLUSIONS

With the reported XPS laboratory data we complete a series of spectroscopic experiments[13,34] on $YbInCu_4$ with varying information depth of the order of $>$1000, 90, and 12 Å for XAS, XPS ($4f$ and $4d$), and UPS, respectively. The changes observed in the spectral features of the Yb $4f$ states in the valence band and the $4d$ core level of the XPS data unambiguously show a first-order valence phase transition and thus—together with the existing data from XAS and UPS—corroborate the previously observed existence of a distorted subsurface zone.[13,17] This indicates a possible explanation for the observed discrepancy in the experimental results and interpretation on various intermediate valent Yb compounds[43,46,49–53] using different excitation energies. High energy spectroscopic techniques using synchrotron radiation (RIXS, XAS, HXPS) are very well suited for the investigation of the bulk properties of surface sensitive solids. On the other hand, the high resolution UPS experiments allow us to detect valuable details in the valence band of these systems, where, however, care has to be exercised in order to separate surface from bulk properties of the spectra.

ACKNOWLEDGMENTS

This work was supported by the Deutsche Forschungsgemeinschaft (Grant Nos. HU 149/19-1 and RE 1469/1) and the Sonderforschungsbereich 277.

*Corresponding author. Email: sw.schmidt@mx.uni-saarland.de

[1] J. W. Allen and R. M. Martin, Phys. Rev. Lett. **49**, 1106 (1982).
[2] J. W. Allen and L. Z. Liu, Phys. Rev. B **46**, 5047 (1992).
[3] L. Z. Liu, J. W. Allen, O. Gunnarsson, N. E. Christensen, and O. K. Andersen, Phys. Rev. B **45**, 8934 (1992).
[4] I. Felner and I. Nowik, Phys. Rev. B **33**, 617 (1986).
[5] E. V. Sampathkumaran, N. Nambudripad, S. K. Dhar, R. Vijayaraghavan, and R. Kuentzler, Phys. Rev. B **35**, 2035 (1987).
[6] J. L. Sarrao, A. P. Ramirez, T. W. Darling, F. Freibert, A. Migliori, C. D. Immer, Z. Fisk, and Y. Uwatoko, Phys. Rev. B **58**, 409 (1998).
[7] I. Felner *et al.*, Phys. Rev. B **35**, 6956 (1987).
[8] B. Kindler, D. Finsterbusch, R. Graf, F. Ritter, W. Assmus, and B. Lüthi, Phys. Rev. B **50**, 704 (1994).
[9] J. L. Sarrao, C. D. Immer, C. L. Benton, Z. Fisk, J. M. Lawrence, D. Mandrus, and J. D. Thompson, Phys. Rev. B **54**, 12207 (1996).
[10] J. M. Lawrence, G. H. Kwei, J. L. Sarrao, Z. Fisk, D. Mandrus, and J. D. Thompson, Phys. Rev. B **54**, 6011 (1996).
[11] A. Löffert, S. Hautsch, F. Ritter, and W. Assmus, Physica B **259-261**, 134 (1999).
[12] There exist two "types" of $YbInCu_4$ with transition temperatures of $T_a \approx 42$ K and $T_a \approx 52$ K. These different transition temperatures result from slightly different stoichiometries. As far as is known, the two types of samples show no differences in their physical properties beyond the different transition temperatures.
[13] F. Reinert, R. Claessen, G. Nicolay, D. Ehm, S. Hüfner, W. P. Ellis, G.-H. Gweon, J. W. Allen, B. Kindler, and W. Assmus, Phys. Rev. B **58**, 12808 (1998).
[14] A. J. Arko, J. J. Joyce, J. Sarrao, Z. Fisk, J. L. Smith, J. D. Thompson, M. Hundley, A. Menovsky, A. Tahvildar-Zadeh, and M. A. Jarell, in *Electron Correlations and Materials Properties*, edited by A. Gonis, N. Kioussis, and M. Ciftan, Proceedings of the First International Workshop on Electron Correlations and Materials Properties (Kluwer Academic/Plenum, New York, 1999), pp. 33–58.
[15] H. Sato *et al.*, J. Synchrotron Radiat. **9**, 229 (2002).
[16] A. L. Cornelius, J. M. Lawrence, J. L. Sarrao, Z. Fisk, M. F. Hundley, G. H. Kwei, J. D. Thompson, C. H. Booth, and F. Bridges, Phys. Rev. B **56**, 7993 (1997).
[17] S. Ogawa, S. Suga, M. Taniguchi, M. Fujisawa, A. Fujimori, T. Shimizu, H. Yasuoka, and K. Yoshimura, Solid State Commun. **67**, 1093 (1988).
[18] M. E. Dávila, S. L. Molodtsov, M. C. Asensio, and C. Laubschat, Phys. Rev. B **62**, 1635 (2000).
[19] E. Weschke, A. Höhr, G. Kaindl, S. L. Molodtsov, S. Danzenbächer, M. Richter, and C. Laubschat, Phys. Rev. B **58**, 3682 (1998).
[20] H. L. Davis, J. B. Hannon, K. B. Ray, and E. W. Plummer, Phys. Rev. Lett. **68**, 2632 (1992).
[21] D. L. Adams and C. S. Sørensen, Surf. Sci. **166**, 495 (1986).
[22] A. Sekiyama, T. Iwasaki, K. Matsuda, Y. Saitoh, Y. Onuki, and S. Suga, Nature (London) **403**, 396 (2000).
[23] S.-H. Yang, S.-J. Oh, H.-D. Kim, R.-J. Jung, A. Sekiyama, T. Iwasaki, S. Suga, Y. Saitoh, E.-J. Cho, and J.-G. Park, Phys. Rev. B **61**, R13329 (2000).
[24] S. Suga and A. Sekiyama, J. Electron Spectrosc. Relat. Phenom. **114-116**, 659 (2001).
[25] T. Iwasaki *et al.*, Phys. Rev. B **61**, 4621 (2000).
[26] T. Matsumoto, T. Shimizu, Y. Yamada, and K. Yoshimura, J. Magn. Magn. Mater. **104-107**, 747 (1992).
[27] K. Kojima, K. Hiraoka, H. Takahashi, N. Môri, and T. Hihara, J. Magn. Magn. Mater. **140-144**, 1241 (1995).
[28] J. M. De Teresa, Z. Arnold, A. del Moral, M. R. Ibarra, J. Kamarád, D. T. Adroja, and B. Rainford, Solid State Commun. **99**, 911 (1996).
[29] C. D. Immer, J. L. Sarrao, Z. Fisk, A. Lacerda, C. Mielke, and J. D. Thompson, Phys. Rev. B **56**, 71 (1997).

[30] J. L. Sarrao, C. L. Benton, Z. Fisk, J. M. Lawrence, D. Mandrus, and J. D. Thompson, Physica B **223&224**, 366 (1996).
[31] S. Tanuma, C. J. Powell, and D. R. Penn, Surf. Interface Anal. **17**, 911 (1991).
[32] A. Jablonski, Phys. Rev. B **58**, 16470 (1998).
[33] A. Jablonski and C. J. Powell, J. Electron Spectrosc. Relat. Phenom. **100**, 137 (1999).
[34] F. Reinert, R. Claessen, G. Nicolay, D. Ehm, S. Hüfner, W. P. Ellis, G.-H. Gweon, J. W. Allen, B. Kindler, and W. Assmus, Phys. Rev. B **63**, 197102 (2001).
[35] C. Dallera, M. Grioni, A. Shukla, G. Vankó, J. L. Sarrao, J. P. Rueff, and D. L. Cox, Phys. Rev. Lett. **88**, 196403 (2002). The absolute values for $n_h(T)$ given in this work have been adjusted to the $n_h(T)$ values obtained by XAS (Ref. 7).
[36] H. Sato *et al.*, Phys. Rev. Lett. **93**, 246404 (2004).
[37] G. K. Wertheim, J. Electron Spectrosc. Relat. Phenom. **15**, 5 (1979).
[38] F. Gerken, J. Phys. F: Met. Phys. **13**, 703 (1983).
[39] S.-J. Oh *et al.*, Phys. Rev. B **37**, 2861 (1988).
[40] M. Okusawa, E. Weschke, R. Meier, G. Kaindl, T. Ishii, N. Sato, and T. Komatsubara, J. Electron Spectrosc. Relat. Phenom. **78**, 139 (1996).
[41] S.-J. Oh, Physica B **186-188**, 26 (1993).
[42] J. M. Lawrence, G. H. Kwei, P. C. Canfield, J. G. DeWitt, and A. C. Lawson, Phys. Rev. B **49**, 1627 (1994).
[43] L. H. Tjeng *et al.*, Phys. Rev. Lett. **71**, 1419 (1993).
[44] B. D. Padalia, W. C. Lang, P. R. Norris, L. M. Watson, and D. J. Fabian, Proc. R. Soc. London, Ser. A **354**, 269 (1977).
[45] H. Ogasawara, A. Kotani, and B. T. Thole, Phys. Rev. B **50**, 12332 (1994).
[46] D. P. Moore, J. J. Joyce, A. J. Arko, J. L. Sarrao, L. Morales, H. Höchst, and Y. D. Chuang, Phys. Rev. B **62**, 16492 (2000).
[47] *The Nature of the Surface Chemical Bond*, edited by T. N. Rhodin and G. Ertl (North-Holland, Amsterdam, 1979).
[48] P. Weibel, M. Grioni, D. Malterre, B. Dardel, Y. Baer, and M. J. Besnus, Z. Phys. B: Condens. Matter **91**, 337 (1993).
[49] J. J. Joyce, A. J. Arko, A. B. Andrews, and R. I. R. Blyth, Phys. Rev. Lett. **72**, 1774 (1994).
[50] J. J. Joyce *et al.*, Physica B **205**, 365 (1994).
[51] J. J. Joyce, A. B. Andrews, A. J. Arko, R. J. Bartlett, R. I. R. Blyth, C. G. Olson, P. J. Benning, P. C. Canfield, and D. M. Poirier, Phys. Rev. B **54**, 17515 (1996).
[52] T. Susaki *et al.*, Phys. Rev. Lett. **77**, 4269 (1996).
[53] J. J. Joyce and A. J. Arko, Phys. Rev. Lett. **78**, 1831 (1997), comment to Ref. 52.